basin connected southward with the Molise Basin.
Within this mosaic, phosphate hardgrounds may provide additional insight in the reconstruction of the deep currents as they are thought to be the product of upwelling and deep nutrient-enriched currents (Burnett et al., 1983; Föllmi, 1996; Föllmi et al., 2008; 2015; Vescogni et al., 2018; Brandano et al., 2016b; 2020). Lower Miocene phosphate rich intervals occur in Malta and Sicily (Pedley and Bennet, 1985; Föllmi et al., 2008), and in the Majella (Mutti and Bernoulli, 2003).

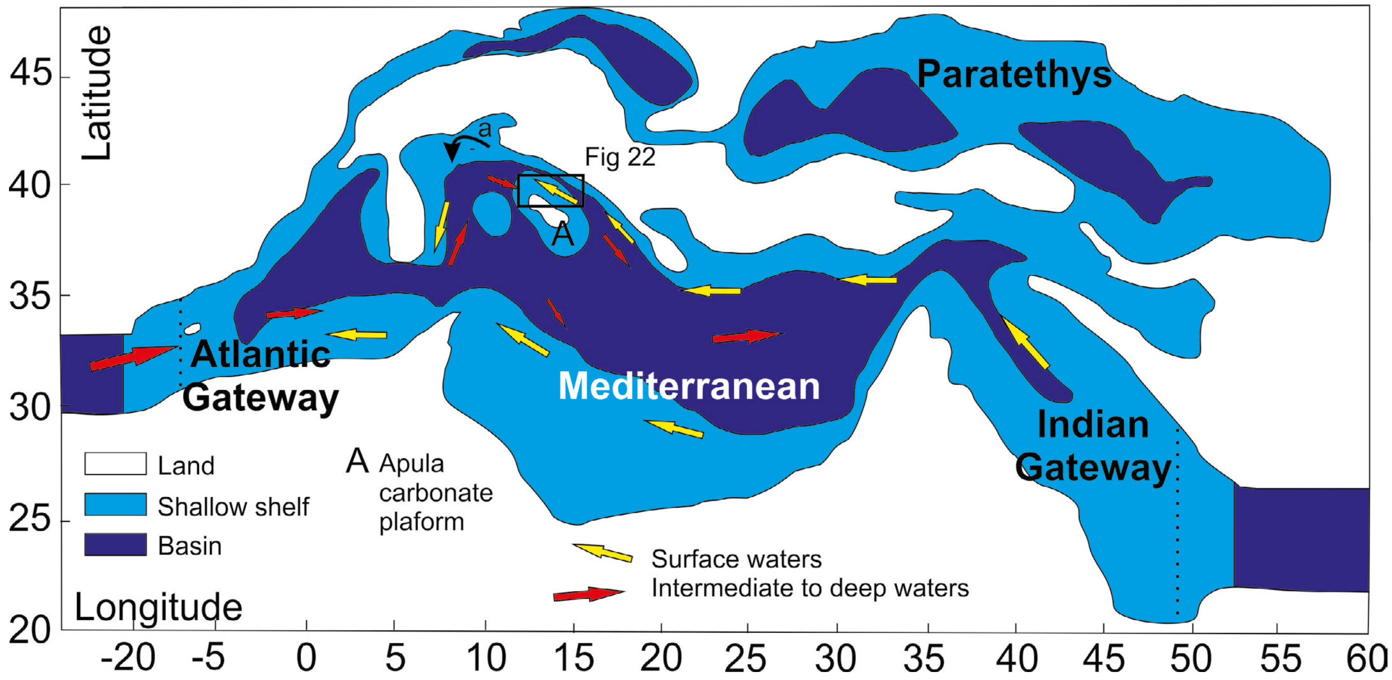

Fig. 6: Paleogeography of the Mediterranean area during Burdigalian.

Oil shows and Bitumens in the Majella Area

During the second half of the XIX century the Majella area represented the vanguard of the Italian oil industry (Jervis, 1873; Magini, 1977; Novelli and Sella, 2009; Gerali and Lipparini, 2018). Moreover, this area has been severely exploited during the early twentieth century, being at that time, the second-largest oil district in Italy after the Emilia Romagna region (Gerali, 2013). From the petroleum system point of view, the Northern sector of the Majella Mountain presents all the needed elements: the source is represented by the Late Triassic-Early Liassic carbonates/evaporites (Cazzini et al., 2015); the reservoir is mainly represented by the carbonate-ramp sequence developed over the Cretaceous platform and its slope (Agosta et al., 2010; Brandano et al., 2013; Scrocca et al., 2013; Lipparini et al., 2018); the seal is represented by both marly levels within the Bolognano Fm (Brandano et al., 2013; Lipparini et al., 2018; Trippetta et al., 2020) and by the Messinian Evaporites (Iadanza et al., 2015) whereas overburden rocks are represented by the overlying younger formations.

In the whole NW sector of the Majella massif, several near-surface and outcropping reservoirs are found locally filled with hydrocarbons at different stratigraphic levels such as the Bolognano Fm reservoirs (Oligocene–Miocene; Scrocca et al., 2013), and also within the carbonates of the Santo Spirito (Paleocene–Oligocene) and Orfento (Upper Cretaceous) Fms. Hydrocarbons, mainly as bitumen, saturates both the rock's matrix and fractures, in particular within the high-porosity carbonates of the Bolognano Fm (Vecsei and Sanders, 1999). Moreover, further to the North, the same saturated reservoir rock (on average at less than 1 km depth) has been greatly investigated and exploited, within the Vallecupa and Cigno oil fields (ViDEPI Project, 2012).

Different interpretations for the oil distribution over the whole NW sector of the Majella area have been proposed in the literature. Based on the structural interpretation of the northern Majella Mountain and the fault architectures, Agosta et al. (2009) suggested that the major faults formed the prime pathways to subsurface fluid flow, assessing that hydrocarbons were channeled along these faults at certain depths, then migrated upward mainly within the deformed carbonates at the extensional jogs of interacting oblique

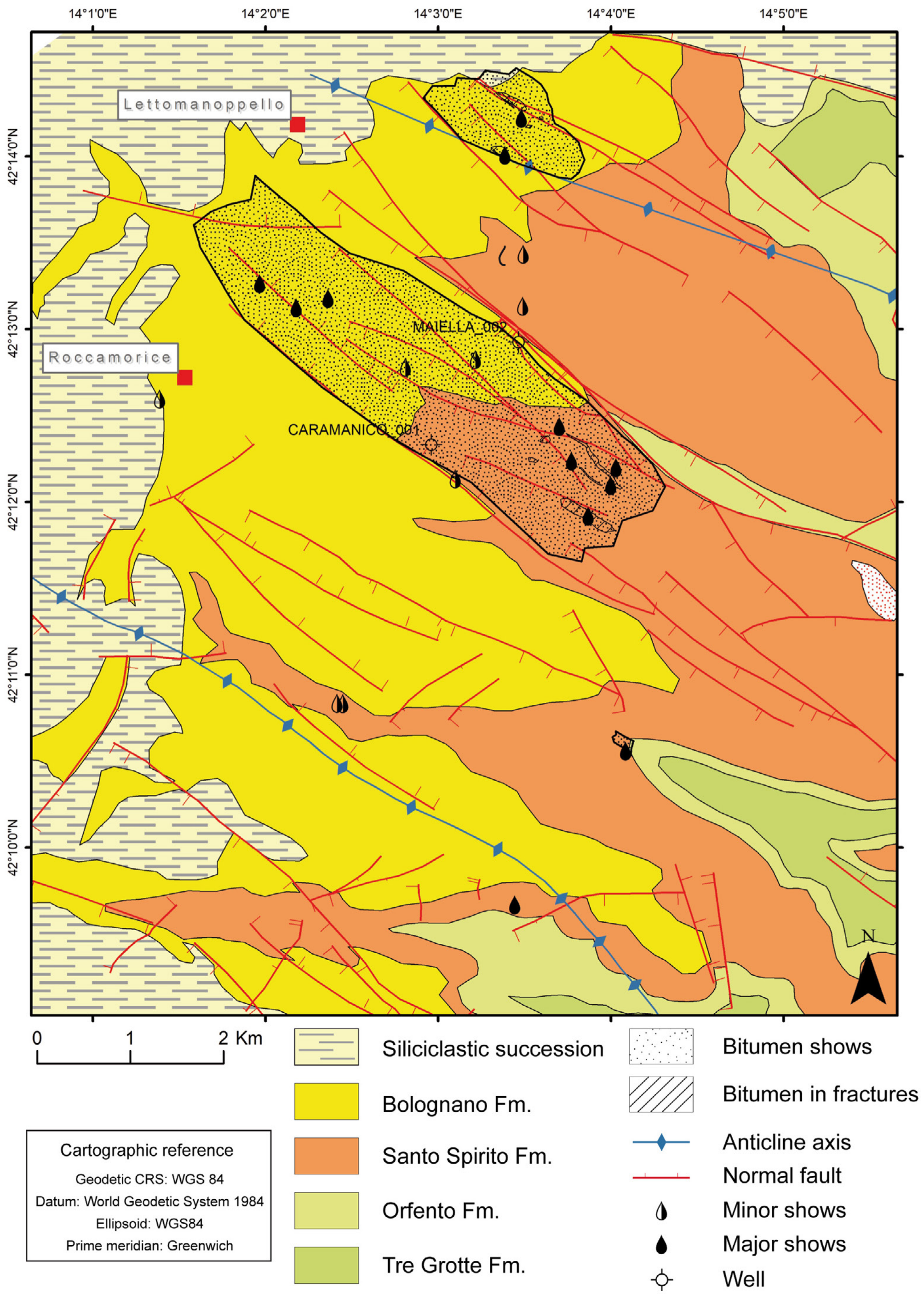

Fig. 7: Simplified geological map showing the distribution of bitumens and the location of the two exploration wells drilled in the study area (modified from Vezzani and Ghisetti, 1998 and Brandano et al., 2013).

normal faults. Lipparini et al. (2018), however, by means of a dataset of shallow wells drilled in two areas, observed that most of the faults do not influence significantly the hydrocarbon presence and its saturation, suggesting for this area a minor role of faults in the hydrocarbon migration.

From a purely geometrical point of view, the hydrocarbon distribution over the area follows an almost NW–SE-oriented trend (Fig. 7), in accordance with the NW–SE-dominating fault trend observed nowadays in the outcrops (e.g. Vezzani and Ghisetti, 1998). This can be related to the capacity of a major NW–SE fault to limit the extension of hydrocarbon occurrence, as suggested by the Piano delle Cappelle main fault. This fault appears today as a sealing fault, related to either the lateral juxtaposition of low-porosity units caused by the large displacement (ca. 180 m), or the possible sealing properties of the fault core, as confirmed by the absence of oil within the cemented fault-breccia.

DAY 1

On this day, we will focus on the general stratigraphic and tectonic setting of the Majella Mountain from the Blockhaus panoramic point (Fig. 1). Successively, we will analyse the stratigraphic architecture of the Bolognano carbonate ramp (Fig. 4). Starting from the north-western sectors, in particular in the Orfento valley, we will then cross the S. Bartolomeo valley to arrive in the eastern sectors, which will be analysed during the second day of the field trip. In the Orfento Valley, we will observe the detail of the stratigraphic succession in the Decontra section, while in the panoramic view of the area between the Giumentina and the S. Bartolomeo Valleys it will be possible to observe the vertical and lateral changes of the Bolognano Fm lithostratigraphic units, which correspond to the environmental and climatic changes occurred between the late Oligocene and the middle Miocene.

Stop T6.1.1
Panoramic view of Majella Carbonate Platform from Blockhaus and Monte Cavallo (42°08’42.21’’N, 14°06’39.76’’E)

The panoramic view from Blockhaus allows recognizing the main stratigraphic architecture of the platform and the transition to the adjacent basin (Fig. 8). The platform can be subdivided into a Lower Cretaceous portion (Monte Pacentro Fm) separated from the Upper Cretaceous portion (Cima delle Murelle Fm) by an unconformity evidenced by karst features and bauxite deposits, ranging from late Albian to early Cenomanian in age (Vecsei et al., 1998). This unconformity is associated with a 5° tilt that can be related to the onset of the extensional tectonic activity in the Late Cretaceous in this part of the Adriatic plate (Vitale et al., 2017; Eberli et al., 2019). Another exposure of the platform occurred during the early to middle Campanian, and concluded the shallow-water platform aggradation phase. The platform margin is cut by a steep and incised escarpment. This escarpment displays a scalloped geometry indicating significant sub-marine erosional processes occurring during platform margin growth. The margin was also segmented along strike orientation and characterised by highs and lows. The depression next to the Monte Rotondo corresponds to the ‘drowning seaway’ of Rusciadelli et al. (2003) and to the ‘Rotondo Channel’ of Eberli et al. (2019). The escarpment is onlapped in the lower part by redeposited bioclastic calcarenites of Valle dell’Inferno unit (Cenomanian) and by magabreccias, bioclastic calcarenites and pelagic limestones of Tre Grotte Fm (Turonian to early Campanian). This onlap is spectacularly visible in the upper part of Valle dell’Orfento from the Monte Cavallo panoramic point. During the Campanian-Maastrichtian, the calcarenites

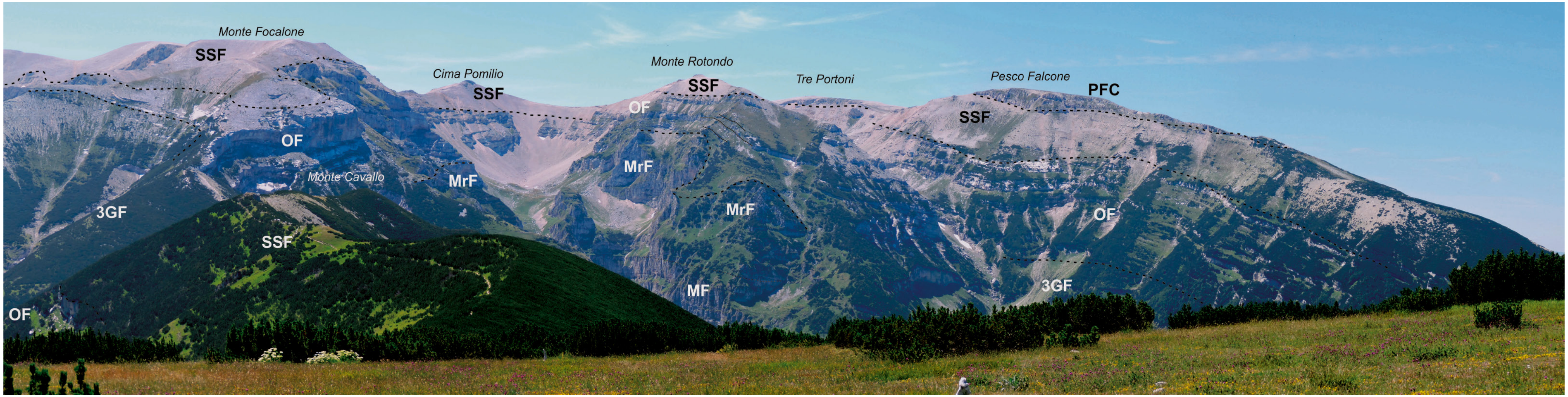

Fig. 8: Panoramic view of the Majella stratigraphic architecture from the Blockhaus, MF = Morrone Fm (Late Jurassic – Early Cretaceous), MrF = Cima delle Murelle Fm. (early Cenomanian–late Campanian), 3GF = Tre Grotte Fm (late Turonian–late Campanian), OF = Orfento Fm (late Campanian–Maastrichtian), SSF = Santo Spirito Fm (Danian-Rupelian), PFC = Pesco Falcone Coral clusters (Rupelian).

of the Orfento Fm prograded over the former basin filled by resedimented sediments shed by the platform since the Turonian until the beginning of the Campanian. The progradation is well observable along the slope of Monte Falcone. The Monte Cavallo point offers a beautiful view of the wedge-shaped geometry of the Orfento Fm delta drift *sensu* Eberli et al. (2019; Fig. 8). The overlying deposits of the S. Spirito Fm (Danian-Bartonian) consist of outer ramp lithofacies represented by a bioturbated, fine, planktonic-rich packstone to wackestone, a bioclastic floatstone alternating with breccias and a bioclastic floatstone to rudstone rich in larger benthic foraminifera. Another unconformity, once again produced by the emersion of the platform, marks the contact between the S. Spirito Fm and the large coral mounds of the Monte Pesco Falcone Fm (Vecsei et al., 1998, Vecsei and Sanders, 1997; Brandano et al., 2019). This unconformity represents the sedimentary record of the sea-level drop of several tens of meters occurred during the Eocene to Oligocene transition (Brandano et al., 2019). The coral bioconstructions developed in a middle ramp environment where luxurious corals built up discrete structures as mounded cluster reefs (Fig. 8). The coral bioconstructions grew seaward of the euphotic seagrass zone. During sea-level rises and following highstands, the cluster reefs coalesced to form an extensive coral unit that prograded for some kilometers toward the basin and interfingered with the outer ramp deposits (Brandano et al., 2019).

https://doi.org/10.3301/GFT.2020.05

Stop T6.1.2
Valle dell'Orfento, the Decontra stratigraphic sections (42°09'46.78''N; 14°02'21.80''E)

The Decontra stratigraphic section is observable in the upper part of Orfento Valley, along the path from Decontra village to Serra S. Antonio (Fig. 9). The base of the section consists of 32 m of the first stratigraphic unit, the

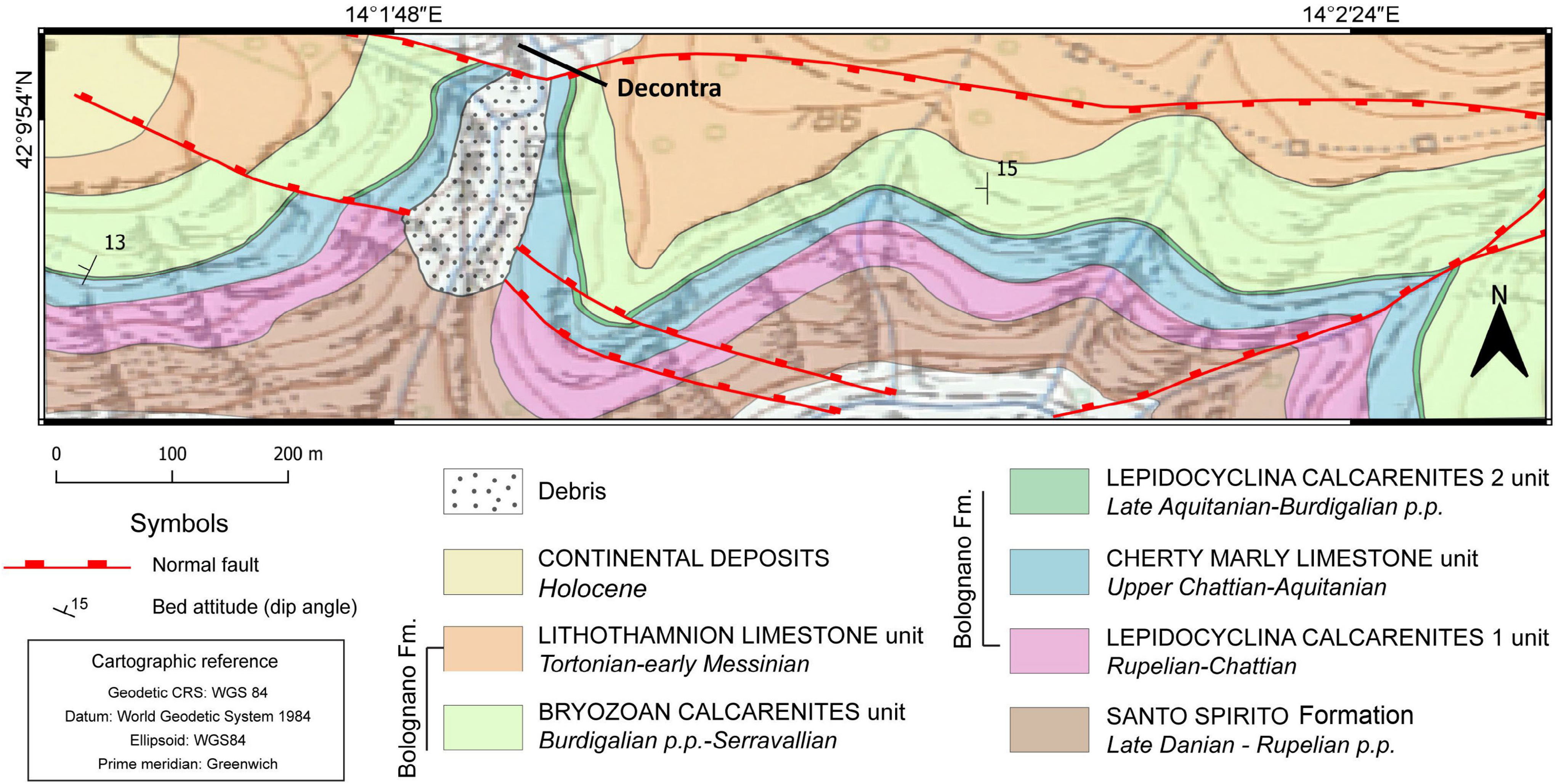

Fig. 9: Geological map of Decontra area.

Lepidocyclina Calcarenite 1 (Figs. 10, 11). This unit is mostly represented by cross-bedded calcarenites consisting of grainstones to packstones with larger benthic foraminifers (LBF) (Fig. 5A, C, D). The main components are in fact *Nephrolepidina*, *Eulepidina*, *Heterostegina* and *Operculina*. Other common components are small benthic foraminifers (SBF) such as rotaliids, *Rotalia*, *Neorotalia viennoti*, *Lobatula lobatula*, *Lenticulina*, *Planorbulina*, discorbaceans, buliminaceans, textularids, and rare miliolids. Red algal debris and bryozoan fragments are frequent, while minor components are *Ditrupa*, echinoid and bivalve fragments and planktonic foraminifera. Two main types of cross-bedding can be recognised in this unit, planar cross-bedding and cuneiform to sigmoidal-shaped cross-bedding (Brandano et al., 2012). LBF biostratigraphy allowed to ascribe this unit at the SBZ22a of Cahuzac and Poignant (1997), therefore to the Rupelian-Chattian stratigraphic interval (Benedetti et al., 2010). The *Lepidocyclina* Calcarenite 1 are overlain by 23.5 m of the cherty bioturbated packstone to wackestone, and nodular bioclastic wackestone to packstone with SBF and bryozoan fragments. Glauconite is common. Age constraints are provided by calcareous nannofossil biostratigraphy. The base of the cherty marly limestones has been attributed to the upper Chattian while the top of the unit is the upper Aquitanian (Brandano et al., 2016a). The Cherty marly limestones are overlain by the *Lepidocyclina* Calcarenite 2, which

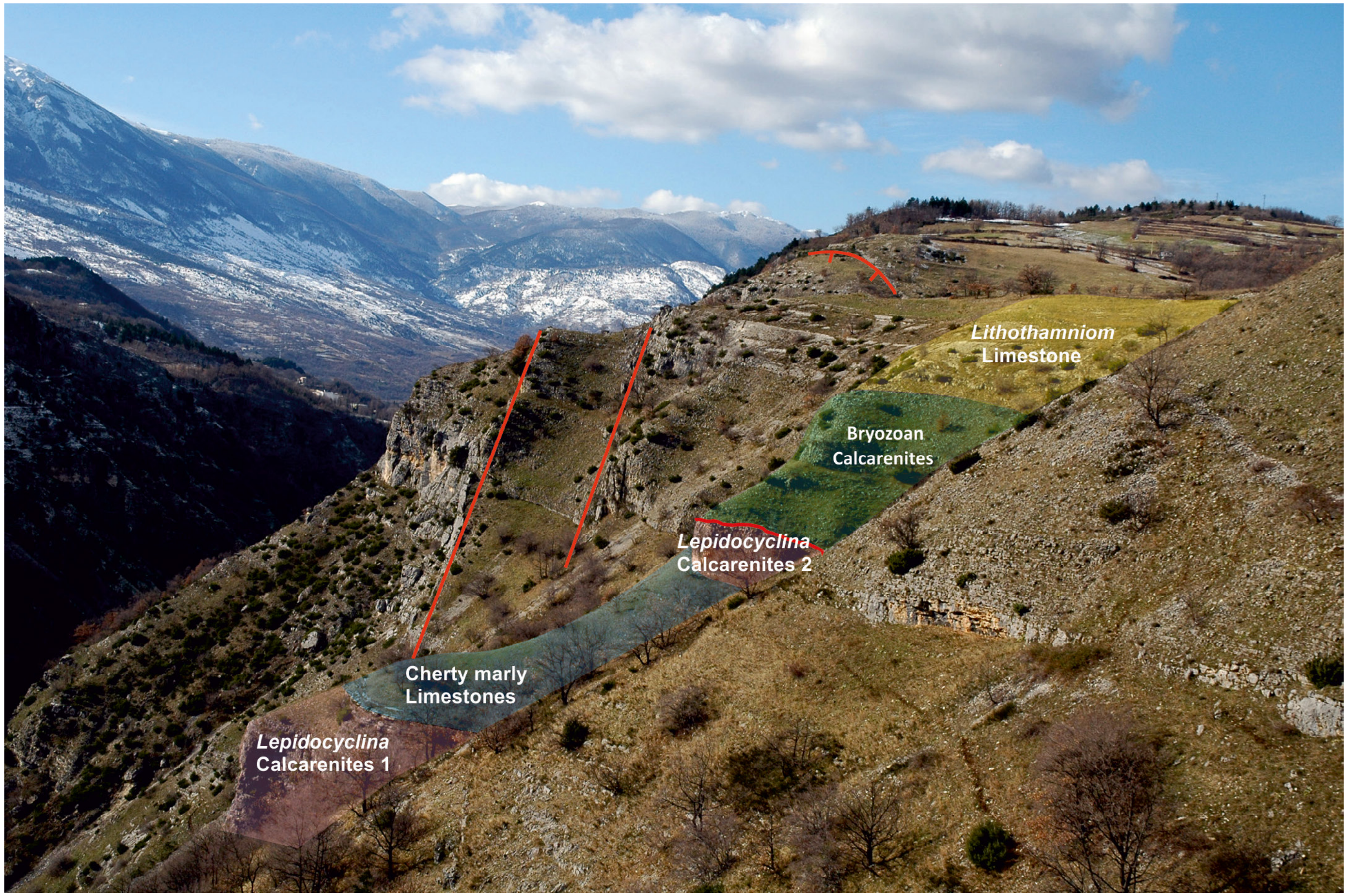

Fig. 10: Panoramic view of Decontra stratigraphic section with photomapping of the main lithostratigraphic units of Bolognano Fm cropping out in the Orfento Valley.

https://doi.org/10.3301/GFT.2020.05

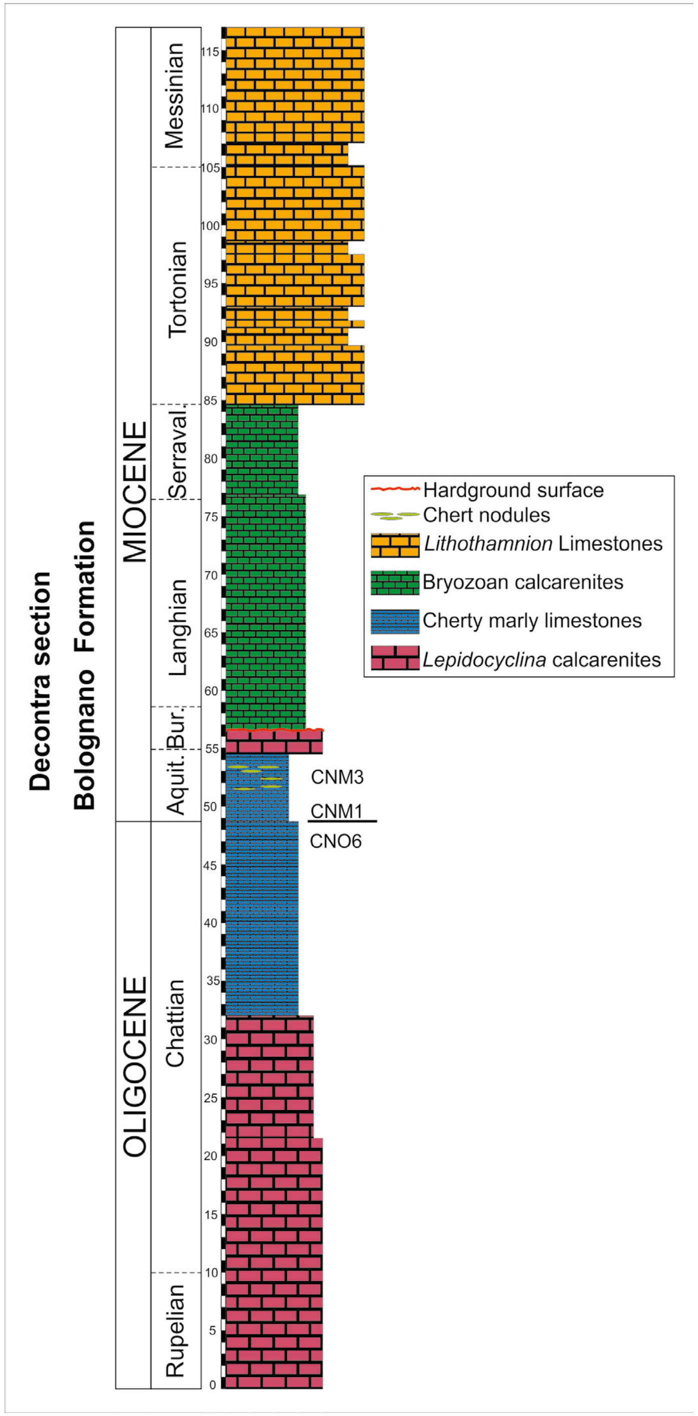

are strongly reduced in the Orfento Valley, they are in fact only 2 m thick and are represented by a bryozoan floatstone. A phosphatic hardground, identified over the entire Bolognano ramp, marks the drowning of the *Lepidocyclina* Calcarenite 2 (Mutti and Bernoulli, 2003). Above the hardground, 28 m of bryozoan calcarenites lie. These calcarenites consist of bioclastic packstones dominated by bryozoan and echinoid fragments (Fig. 5E, Fig. 11). This lithofacies is characterized by planar to trough cross-bedding. The beds are 0.2 to 0.6 m thick and they are separated by marly layers of few cm in thickness. The overlaying unit, the *Lithothamnion* limestone, lies unconformably on the Bryozoan calcarenites. The base of this unit is marked by a 1.5 m thick *Heterostegina* level (Fig. 5G), followed upward by 33.5 m of thick-bedded red algae packstones and free living red algae rudstones to floatstones (Fig. 5H). The skeletal assemblages are dominated by larger benthic foraminifers (*Amphistegina*, *Operculina* and *Heterostegina*), smaller benthic foraminifers (*Elphidium*, rotalids), bryozoans, bivalve fragments, vermetid tubes, and echinoid fragments. Three different stages in the evolution of this unit can be recognized. During the first stage, the ramp was subjected to high-energy wave-dominated conditions. In the second stage, coralline algal (mäerl) facies and seagrass meadows developed, initially in an oligotrophic setting, later followed by a slight reduction in light penetration. The third stage involved a general increase in fine terrigenous sediments, together with a further decrease in light and also by the spread of coralline algal bindstone facies. The elevated terrigenous input was associated with increased trophic conditions, as also shown by the occurrence of abundant plankton and low-oxygenated foraminiferal assemblages (Brandano et al., 2016c). The base of the *Lithothamnion*

Fig. 11: Stratigraphic log of Decontra section and chronostratigraphy and lithostratigraphy of Bolognano Fm (after Brandano et al., 2016a).

limestones has been ascribed to the Tortonian by means of Sr Isotope stratigraphy, while the upper portion of this unit is Messinian in age due to the occurrence of the small benthic foraminifer marker *Bulimina echinata* (Patacca et al., 2008; Cornacchia et al., 2017).

Stop T6.1.3
Panoramic view of S. Bartolomeo Valley (42°10'52.70''N; 14°02'05.61''E)

The panoramic view from the southern side of S. Bartolomeo Valley provides a spectacular view of the Bolognano Fm stratigraphic architecture (Fig. 12). The view shows two calcareous lithostratigraphic units separated by a marly unit (Fig. 13). The debris of the marly unit result in scree-producing elements, while the limestones of the *Lepidocyclina* units form weather resistant cliffs. The basal unit is represented by *Lepidocyclina* Calcarenite 1 that overlies the Eocene carbonates of the S. Spirito Fm. Here the thickness of this unit is 53 m. The

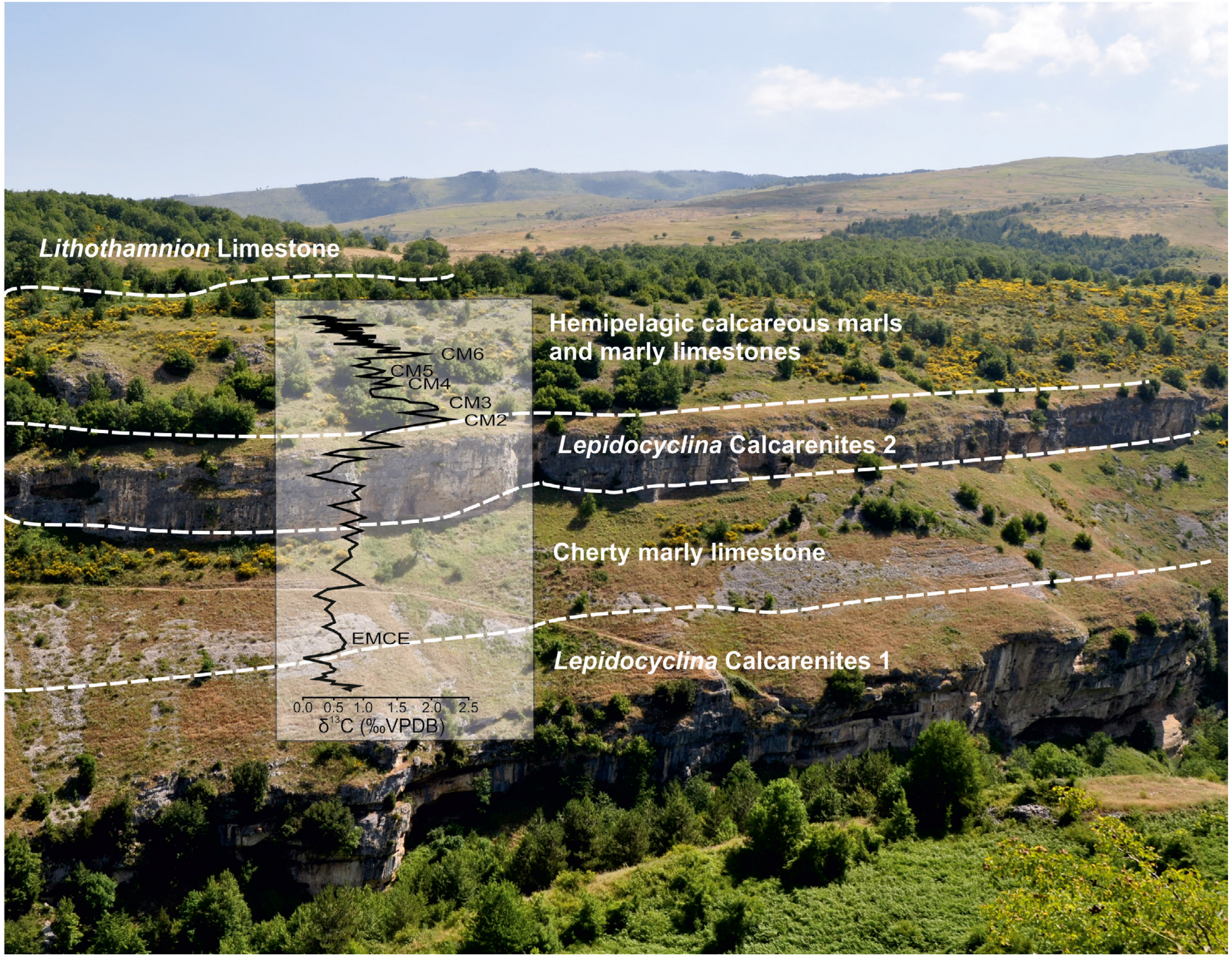

Fig. 12: Panoramic view of the S. Bartolomeo Valley with photomapping of the main lithostratigraphic units of the Bolognano Fm and the relative C-isotope curve from Brandano et al. (2017).

https://doi.org/10.3301/GFT.2020.05

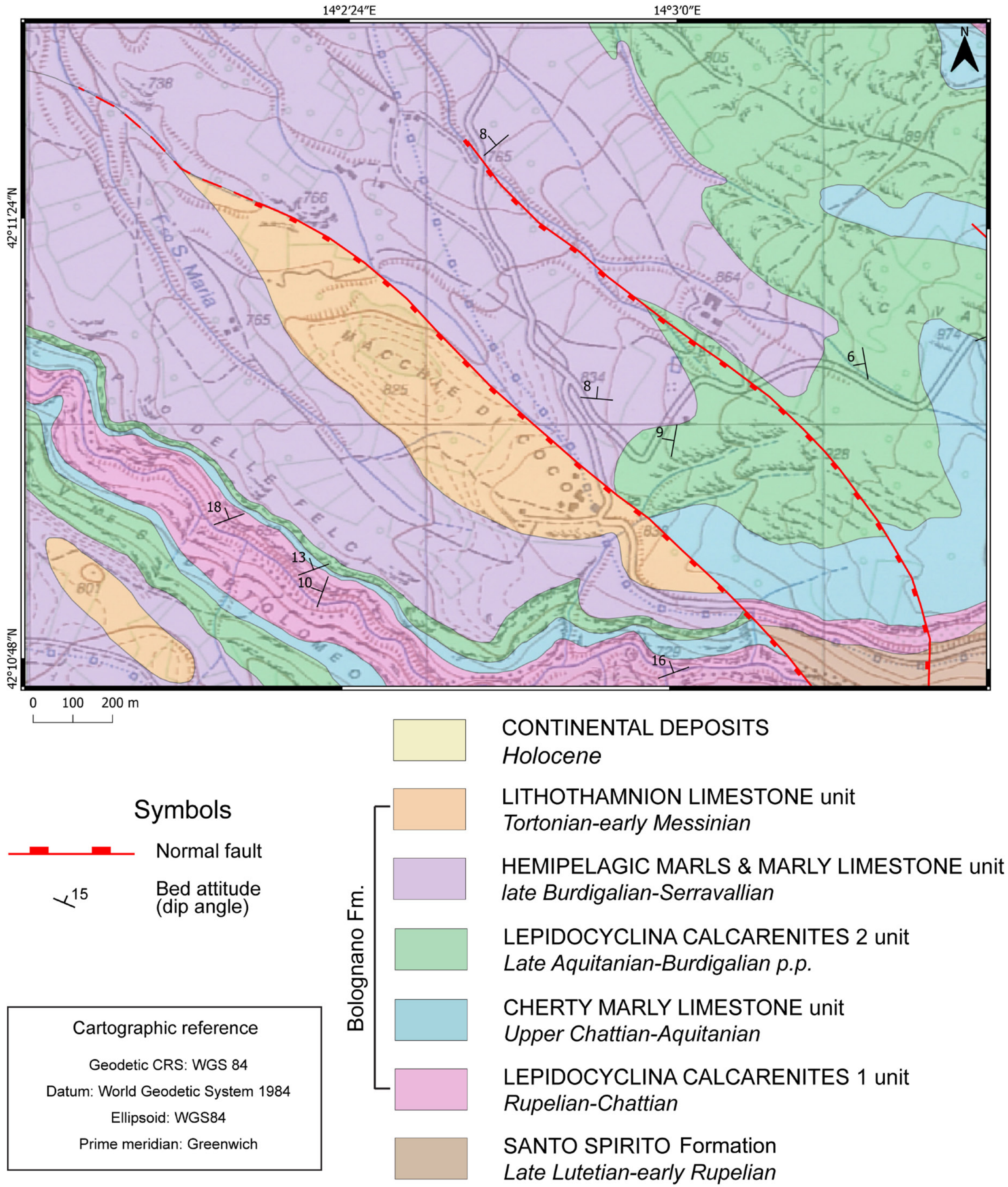

Lepidocyclina Calcarenite 1 are overlain by the cherty marly limestone unit, 18 m thick, overlain by another cross-bedded calcarenites unit, the *Lepidocyclina* calcarenites 2. The *Lepidocyclina* Calcarenite 2 unit shows compositional and sedimentological characteristics that are similar to those of the basal *Lepidocyclina* Calcarenite 1 unit, except for a decrease in abundance of larger benthic foraminifer specimens. The thickness of this unit in the S. Bartolomeo valley increases up to 16 m with respect to Orfento valley where it was only 2 m thick. In the S. Bartolomeo valley, the *Lepidocyclina* Calcarenite 2 is overlaid by the hemipelagic marls unit instead of the bryozoan calcarenites observed in the Orfento valley (Figs. 4, 9).

In this area, the basal portion of the composite S. Bartolomeo Valley–Orta stratigraphic section has been measured and sampled. This section records the Chattian–Serravallian evolution of the Bolognano Fm. In particular, the section displays a good record of the EMCM (Early Miocene Carbon Maximum) and the Monterey Excursion (Fig. 12). In fact, the carbon isotope record is marked by a minor, but sharp, positive $\delta^{13}C$ shift at the Oligocene-Miocene boundary. This isotopic

Fig. 13: Geological map of S. Bartolomeo area.

shift corresponds to the drowning of the *Lepidocyclina* Calcarenite 1 carbonate ramp, overlain by the Cherty Marly Limestone unit. The increase in $\delta^{13}C$ values reflects an increased productivity of surface seawater. Eutrophic events may have caused the drowning of carbonate platforms due to the shift from photo-dependent-dominated to the filter feeding biota (Mutti and Hallock, 2003). The onset of the Monterey Event in the Bolognano Fm is recorded by the *Lepidocyclina* Calcarenite 2 unit, which is characterized by the abundance of bryozoans and echinoid fragments in place of larger benthic foraminifera. The spread of bryozoans has been linked to an increased nutrient availability in surface waters (Brandano et al., 2010; 2017). Under an enhanced nutrient flux, due to continental runoff or upwelling, phytoplankton blooms may increase the surface water turbidity, thus reducing the light available for the bottom-dwelling organisms, such as the larger benthic foraminifera.

DAY 2

The second day will be focused on the large dune field characterizing the *Lepidocyclina* Calcarenite 2 in the outcrop of Piano delle Cappelle. In the last stops of the field trip we will observe as this unit represents an exhumed part of a petroleum system that was active in the northern part of Majella area. Hydrocarbon occurrences in both matrix and fracture porosity will be observed in detail in the stops of the Acquafredda block and in the Valle Romana Quarry, where beautiful exposure of bitumen shows and seepages are present.

Stop T6.2.1
Piano delle Cappelle – Dune field (42°13’00.21’’N; 14°04’18.17’’E)

The Piano delle Cappelle area is dominated by *Lepidocyclina* Calcarenite 2 (Fig. 14). Along the road leading to the abandoned S. Maria quarry, it is possible to analyse the spectacular sedimentary structures characterizing this unit. The *Lepidocyclina* Calcarenite 2 represents the sedimentation between the oligophotic and the aphotic zone of a carbonate ramp environment affected by high energy currents. The sediment consists mainly of bryozoan colonies (celleporids and adeoniforms) and echinoids. Large benthic foraminifera are common and represented by *Nephrolepidina*, *Amphistegina* and nummulitids. Other minor components are red-algal debris, small benthic foraminifera, serpulid fragments, pectinid fragments, and planktonic foraminifera (Fig. 5A, C, D).
The cross bedding characterizing this unit is produced by the migration of submarine dunes (Fig. 15). In the initial part of the S. Maria Quarry road, the dunes correspond to a more distal sector of the ramp. Here

https://doi.org/10.3301/GFT.2020.05

the palaeocurrent patterns are indicative of a generally basinward, north–west directed flow (Fig. 15A, 16). The dunes show dip azimuth in the range of 290°-320°. The geometries are typical of simple dunes without internal angular discontinuities and compound dunes with one order of discontinuity or, more rarely, two orders in internal organization. The first order sets contain parallel lamination. Foresets are generally tangential, with dip angles decreasing from 20° to few degrees toward the bottomset. Three-dimensional reconstructions of the bedforms were obtained by means of a terrestrial laser scanner (Brandano et al., 2012). The dunes generally show a planar lower bounding-surface shape, with dunes migrating on a flat surface. The height of the dunes ranges from 5 to 9 m, and their average length ranges from about 200 to 300 m. They have

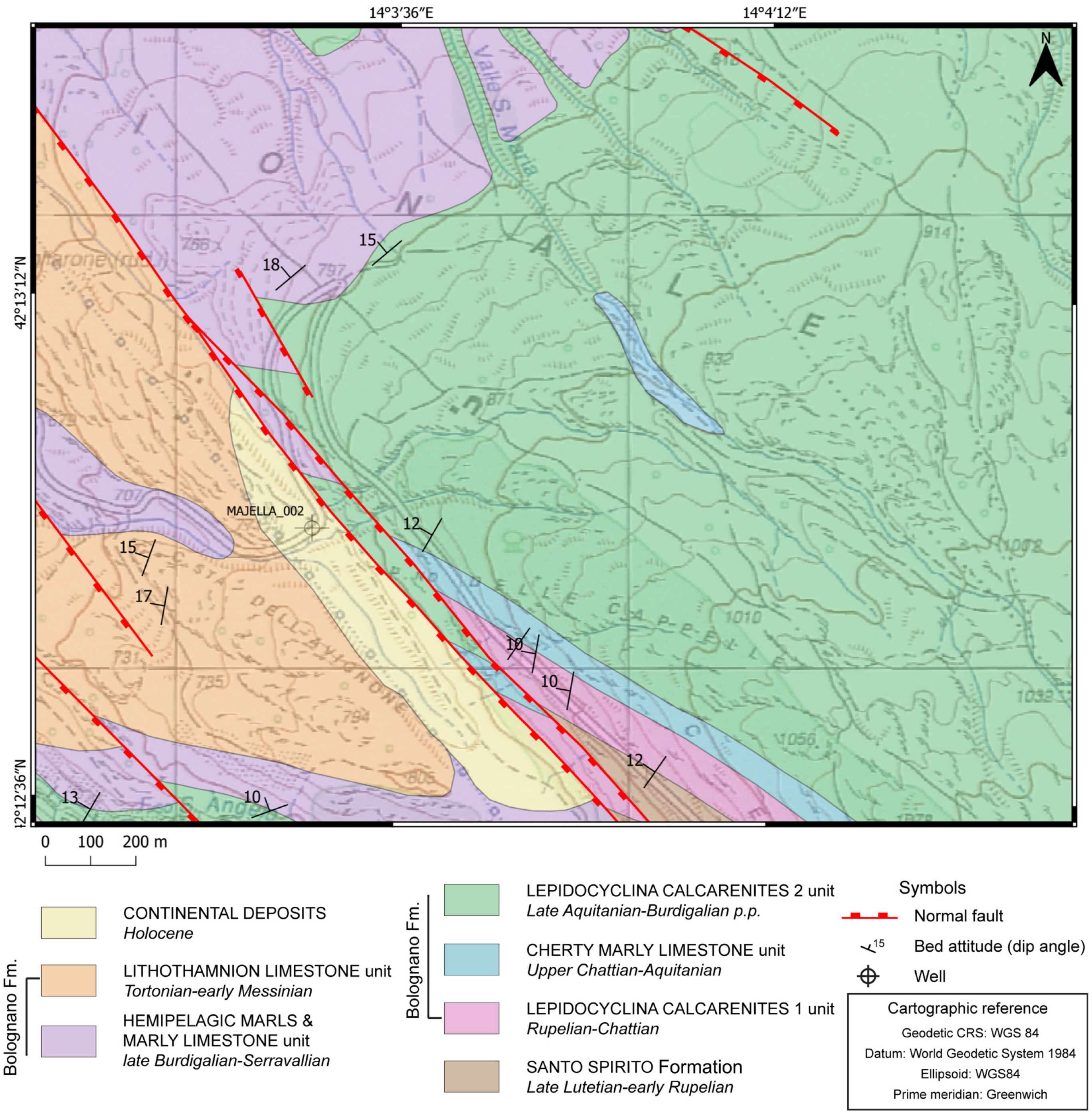

Fig. 14: Geological map of the Piano delle Cappelle area.

Fig. 15: cross-bedding of *Lepidocyclina* Calcarenite 2, A) northwest oriented simple and compound dunes bounded by flat surfaces; B) second order sets of a northeast oriented dune; C) interfingering of northwest and northeast oriented dunes.

https://doi.org/10.3301/GFT.2020.05

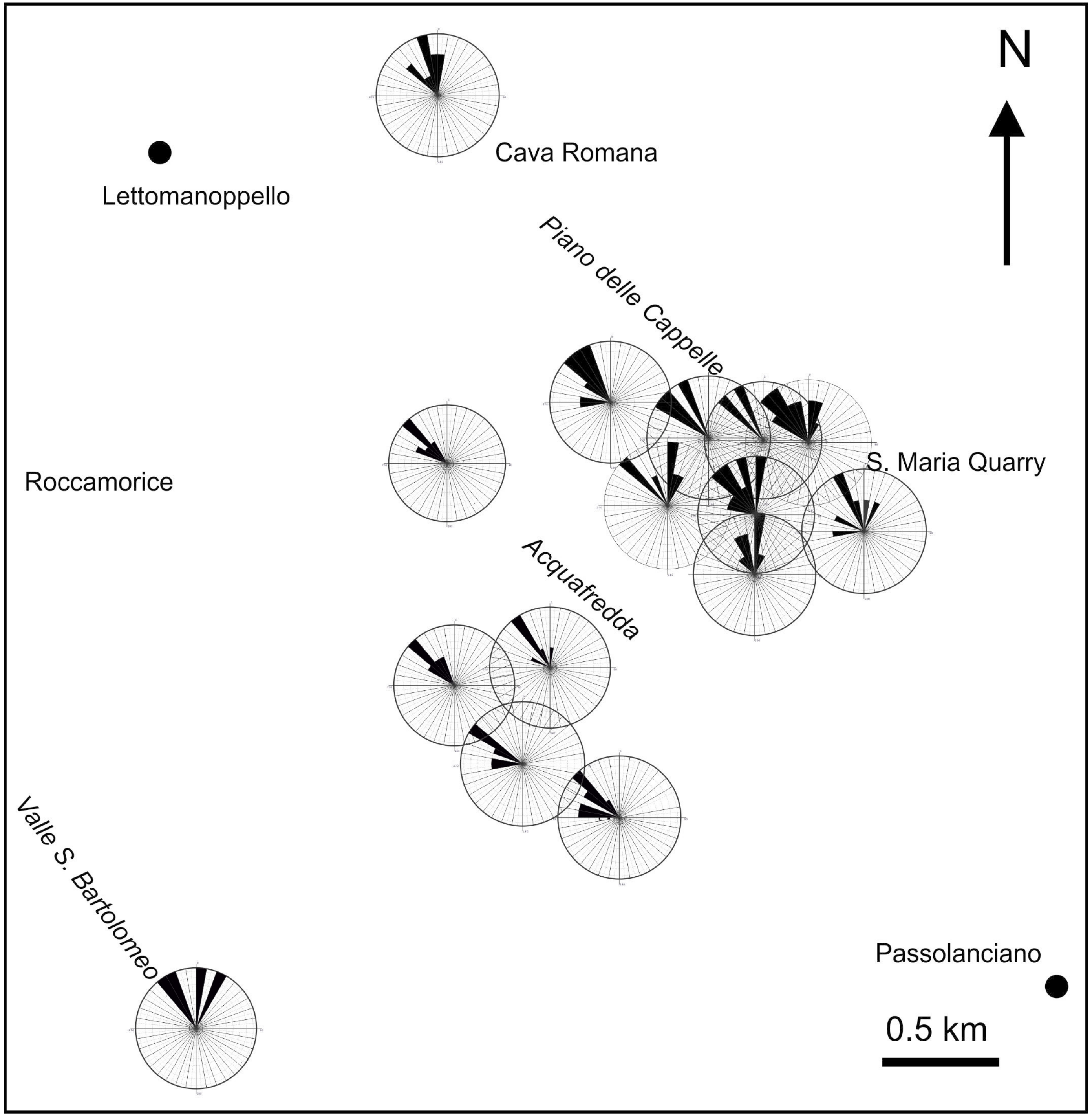

straight or slightly sinuous crests, being considered mainly as 2D and subordinately 3D bedforms (*sensu* Ashley, 1990).
Walking 0.5 km toward the S. Maria quarry, we move toward more proximal environment of the middle ramp. Here the dunes show two main orientations (Fig. 16). A group is still oriented basinward with dip generally toward WNW and they display similar characters to the dunes previously described, the only difference is a reduced height of the composite dunes, up to 3-4 m. A second group of bedforms is perpendicularly oriented with respect the first group (Figs. 15B, C). The dip is generally toward NE of 20° and 10°. The sets are characterized by bedding-parallel lamination, the thickness ranges between 10 and 60 cm. These dunes show a trough-shaped bounding-surfaces, however flat

Fig. 16: Palaeocurrents in the *Lepidocyclina* Calcarenite 2. The generalized regional palaeocurrent direction is toward NW.

https://doi.org/10.3301/GFT.2020.05